

Mode selection mechanism and magnetic diffusivity in a non-axisymmetric solar dynamo model

Jie Jiang and Jingxiu Wang

*National Astronomical Observatories, Chinese Academy of Sciences, Beijing
100012, China E-mail: jiangjie@ourstar.bao.ac.cn*

Abstract

The generation of solar non-axisymmetric magnetic fields is studied based on a linear $\alpha^2 - \Omega$ dynamo model in a rotating spherical frame. The model consists of a solar-like differential rotation, a magnetic diffusivity varied with depth, and three types of α -effects with different locations, i.e. the tachocline, the whole convective zone and the sub-surface. Some comparisons of the critical α -values of axisymmetric ($m = 0$) and longitude-dependent modes ($m = 1, 2, 3$) are presented to show the roles of the magnetic diffusivity in the problem of modes selection. With the changing of diffusivity intensity for the given solar differential rotation system, the dominant mode possibly changes likewise and the stronger the diffusivity is, the easier the non-axisymmetric modes are excited. The influence of the diffusivity and differential rotation on the configurations of the dominant modes are also presented.

Key words: Sun: magnetic fields; Sun: diffusivity; Dynamo theory

1 Introduction

Since Carrington (1863) suspected that sunspots did not form randomly over solar longitudes, many researches were undertaken to investigate the preferred longitudes of solar magnetic field. ‘Active Longitudes’ (Švestka and Simon , 1969), ‘Sunspot Nests’ (Castenmiller et al. , 1986), ‘Hot Spots’ (Bai , 1987) and so on were defined and presented. The well-known ‘flip-flop’ phenomena of late-type stars were also identified on the Sun (Berdugina and Usoskin , 2003). These more and more observational evidences indicate the involvement of non-axisymmetric, i.e. longitude-dependent large-scale magnetic fields in the formation and evolution of solar activities.

Although many papers reported the evidences for the existence of longitudinal inhomogeneities in sunspots distribution, the results were always inconsistent with each other on the number of the active longitudes, i.e. longitudinal wave number m . Altschuler et al. (1974) analyzed the large-scale photospheric magnetic field in terms of surface harmonics and showed that the modes $m \leq 3$ were prominent throughout the solar cycle. de Toma et al. (2000) argued that the total numbers of active regions per rotation per hemisphere varied between 0 and 7. Song and Wang (2005) suggested that 55 percent of the solar magnetic flux can be represented by a mode of $m = 6$ in the northern hemisphere and by $m = 5$ in the southern one. However, the identification of flip-flops on the Sun (Berdyugina and Usoskin , 2003) indicates the mainly non-axisymmetric mode $m = 1$. The ambiguous longitudinal wave numbers may arouse a series of questions. Which kinds of physical mechanisms are responsible for the preferred mode to excite? For each mode, what is its configuration and which ingredients have the primary influence on the configuration? These are the main objectives of the paper.

In order to explain the questions about the non-axisymmetric field of the Sun, it is natural to set up the non-axisymmetric solar dynamo model. There are two basic processes in the traditional $\alpha - \Omega$ dynamo model (Parker , 1955; Steenbeck, krause and Rädler, 1966): (i) the generation of toroidal field by shearing a pre-existing poloidal field (the Ω -effect) and (ii) the re-generation of poloidal field from the toroidal field (the α -effect) . Moreover, meridional circulation is always considered to transport the magnetic flux. The $\alpha - \Omega$ dynamo is the limit of $\alpha^2 - \Omega$ dynamo in which the α -effect is included as a second generation source of the toroidal field. The role of the α -effect and the Ω -effect in dynamo process has been well-researched and well-known. But there is another important ingredient, i.e. the magnetic diffusivity. Except for opposing the generation of magnetic field, what other roles does it play in the non-axisymmetric dynamo process?

Magnetic diffusivity consists of molecular diffusivity and turbulent one. Since turbulent diffusivity is much stronger, we neglect the molecular diffusivity. Yoshimura et al. (1984c) showed that anisotropic turbulent diffusivity is a key factor on parity selection especially for the latitudinal-gradient-dominated differential rotation. Chatterjee et el. (2004) adopted different diffusivity-profiles (scalars) for toroidal and poloidal fields in a two-dimensional solar dynamo model, based on the helioseismically determined solar rotation profile and Babcock-Leighton-type α -effect. The solar-like dipolar parity was obtained. Obviously, the diffusivity has directly relation with the parity selection in dynamo process. In the following, we also regard the diffusivity as a scalar and discuss its influence on the mode selection and magnetic configuration during the non-axisymmetric dynamo process.

In the next section, we set up a linear non-axisymmetric $\alpha^2 - \Omega$ dynamo model

in a rotating frame with solar inner core and introduce the spectral method to numerically solve it. We present the role of turbulent diffusivity as well as the differential rotation by the comparisons of the critical α -value of axisymmetric and longitude-dependent modes, and further show their configurations in Section 3. In Section 4, We give some discussion and conclusions.

2 The Non-axisymmetric Dynamo Model

2.1 The basic equations and numerical scheme

We solve the standard mean field dynamo equation

$$\frac{\partial \mathbf{B}}{\partial t} = \nabla \times [\mathbf{U} \times \mathbf{B} + \alpha \mathbf{B} - \eta \nabla \times \mathbf{B}], \quad (1)$$

in the spherical polar coordinates (r, θ, ϕ) . For the flow field \mathbf{U} , only the (differential) rotation Ω without the meridional circulation is considered for simplicity. η is the magnetic diffusivity. We non-dimensionalize the equation (1) in terms of the length R_\odot and the time R_\odot^2/η_o . Thus Eq. (1) becomes

$$\frac{\partial \mathbf{B}}{\partial t} = R_\Omega \nabla \times (\mathbf{U}'_\phi \times \mathbf{B}) + R_\alpha \nabla \times (\alpha' \mathbf{B}) - \nabla \times (\eta' \nabla \times \mathbf{B}), \quad (2)$$

where $R_\alpha = \frac{\alpha_o R_\odot}{\eta_o}$, $R_\Omega = \frac{|\Omega|_o R_\odot^2}{\eta_o}$. η_o , α_o and $|\Omega|_o$ are the reference values of the diffusivity in the convective zone (CZ), the α -effect and the differential rotation respectively. The quantities R_α and R_Ω are the dynamo numbers measuring the relative importance of inductive versus diffusive effects.

At two interfaces $r = r_o = 1.0$ and $r = r_i = 0.6$ (after non-dimensionalization), both magnetic field and the tangential electric field must be continuous. The exterior $r > 1.0$ is a vacuum and eigensolutions are matched to a potential field. The radiative core is assumed to behave as a perfect conductor (See Schubert and Zhang (2001), Jiang and Wang (2006) for detail).

Since the magnetic field is divergence-free, we expand \mathbf{B} in term of two scalar functions h and g which represent the poloidal and toroidal potentials as (Moffatt , 1978)

$$\mathbf{B} = \nabla \times \nabla \times \mathbf{r}h(r, \theta, \phi, t) + \nabla \times \mathbf{r}g(r, \theta, \phi, t). \quad (3)$$

With given boundary conditions and linear frame, we can look for the eigen-solutions of the equations about h and g with the form

$$[h(r, \theta, \phi, t), g(r, \theta, \phi, t)] = [h(r, \theta, \phi), g(r, \theta, \phi)]e^{st}, \quad (4)$$

where s is the eigenvalue and can be written as $s = \sigma + i\omega$. Only the solutions that neither grow nor decay, i.e. the onset of dynamo actions ($\sigma = 0$) are considered in the paper. For given R_Ω , the corresponding dynamo number R_α is the critical R_α and the corresponding value of α_o is the critical α -value.

Different modes are decoupled in the linear theory. We expand h and g at the onset of the dynamo action in terms of Chebyshev polynomial $T_n(r)$ and surface harmonics $P_l^m e^{im\phi}$ in the meridional circular sector $r \in [0.6, 1.0]$, $\theta \in [0.0, \pi]$ for given m as follows:

$$h = \sum_{n=0}^N \sum_{l=m}^L c_{n,l}^h T_n(ar - b) P_l^m(\cos \theta) e^{im\phi}, \quad (5)$$

$$g = \sum_{n=0}^N \sum_{l=m}^L c_{n,l}^g T_n(ar - b) P_l^m(\cos \theta) e^{im\phi}, \quad (6)$$

where $ar - b \in [-1, +1]$. N and L are the truncation levels to get convergence. It varies with different dynamo numbers and different Ω, η, α profiles. $c_{n,l}^h$ and $c_{n,l}^g$ are eigenvectors.

As pointed out by Ivanova and Ruzmaikin (1985), the system of equations about h and g may be decomposed into two subsystems, i.e. odd or even parity with respect to the equatorial plane denoted by A and S . With the parameters adopted in our model, both odd and even parity solutions have nearly the same critical R_α and actions for given mode m . It should be enough to present one kind of parity for each mode. Since the odd parity for axisymmetric mode $A0$ has been confirmed by the observations, we will discuss it and the opposite parity (even ones) for the non-axisymmetric modes (Sm). Note that, it does not mean there have no possibility for $S0$ and Am existing on the Sun. Through studying the heliospheric magnetic field, Mursula and Hiltula (2004) gave the evidence for $S0$ mode on the Sun. For the non-axisymmetric modes, just like Stix (1971), only the modes $m = 1, 2, 3$ ($S1, S2, S3$) are considered since they are the most interesting ones in view of observational evidences.

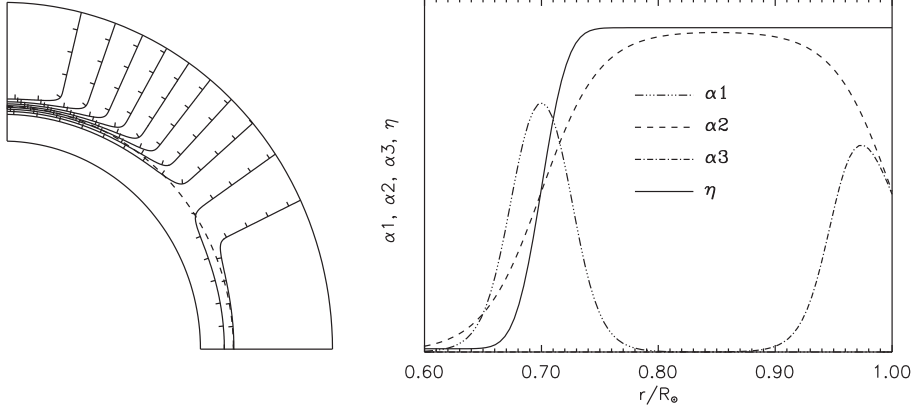


Fig. 1. Left: Contours of constant angular velocity obtained from Eq. (7). The short, perpendicular ticks mark the ‘downhill’ direction. The dashed line denotes the center of the tachocline locating at $0.7R_\odot$. The differential rotation is symmetric about the equator and only quadrant is shown. Right: Radial distributions of the three types of α -effects and the turbulent diffusivity η . Values of y-axis are not scaled.

2.2 Three ingredients in the model

We use the following expression for the solar internal rotation (Schou et al. , 1998; Charbonneau et al. , 1999)

$$\Omega(r, \theta) = \Omega_c + \frac{1}{2} [1 + \text{erf}(2\frac{r - r_c}{w})] (\Omega_s(\theta) - \Omega_c), \quad (7)$$

where $\Omega_s(\theta) = \Omega_{EQ} + a_2 \cos^2 \theta + a_4 \cos^4 \theta$ is the surface latitudinal rotation. The parametric values are set as $r_c = 0.7R_\odot$, $w = 0.05R_\odot$, $\Omega_c/2\pi = 430.0$ nHz, $\Omega_{EQ}/2\pi = 455.8$ nHz, $a_2/2\pi = -51.2$ nHz, $a_4/2\pi = -84.0$ nHz. It closely resembles the best-fit helioseismic solution. Left of Fig. 1 is the contours of constant angular velocity. Within the tachocline, rotation increases with distance from the core at low latitudes, while it decreases at high latitudes. At intermediate latitudes (near 35°), rotation is almost independent on depth. Furthermore, we base our model on the rotating spherical systems with the rotation velocity Ω_c of the inner core. Thus the differential rotation in the rotating frame Ω_c is

$$\Omega'(r, \theta) = (2\pi 25.8) \times \frac{1}{2} [1 + \text{erf}(2\frac{r - r_c}{w})] (1 - 1.98 \cos^2 \theta - 3.26 \cos^4 \theta) \text{ (nHz)}. \quad (8)$$

The surface equatorial differential rotation is $(2\pi 25.8)$ nHz and we regard it as the characteristic value of the differential rotation $|\Omega|_o$. Hence, R_Ω should be equal to $\frac{8 \times 10^{10} \text{ m}^2 \text{s}^{-1}}{\eta_o}$ and be decided only by the reference value of the

diffusivity η_o .

We make the simple assumptions that both α -effect and magnetic diffusivity η are scalars. Whilst bearing in mind that they should be written as tensor quantities in a more realistic model. We use the analytical expression of Dikpati and Charbonneau (1999) for the diffusivity profile as

$$\eta(r) = \eta_c + \frac{\eta_o}{2} [1 + \operatorname{erf}(2\frac{r - r_c}{w})], \quad (9)$$

which can be seen in the right of Fig. 1 (solid line). The diffusivity η_o in CZ, is dominated by its turbulent contribution. In the stably stratified core, the diffusivity η_c is much lower because of the much less turbulence. In the following, we take $\eta_c/\eta_o=0.01$. The transition from high to low diffusivity occurs near the tachocline, which is coincident with the rotational shear layer. Here, η_o is far less definite but is widely known that it ranges from $2 \times 10^{10} \text{ cm}^2\text{s}^{-1}$ to $2 \times 10^{12} \text{ cm}^2\text{s}^{-1}$.

The α -effect cannot yet be determined from observations. We consider three typical cases with different regions it works. They are in the tachocline, the convective zone and the near-surface. We denote them as C1, C2 and C3 respectively. The expression for them can be written as

$$\alpha(r, \theta) = \alpha_o \frac{1}{2} [1 + \operatorname{erf}(\frac{r - r_a}{d})] \frac{1}{2} [1 - \operatorname{erf}(\frac{r - r_b}{d})] \cos \theta. \quad (10)$$

r_a , r_b and d change with different types of α -effects. α_o occurred in the dynamo number R_α also presents the amplitude of the α -effect. The radial profiles are shown in the right of Fig. 1. The common angular dependence $\cos \theta$ is adopted, which is the simplest guaranteeing antisymmetry across the equator. Moreover, we do not consider the α -quenching since only the linear solutions are sought.

3 Numerical results

We perform some numerical explorations with the above three different α -profiles. In order to reveal the ingredients contributing to the mode selection, we test R_Ω at the values of 500, 2000 and 5000 and accordingly, the typical values of diffusivity are $1.6 \times 10^{12} \text{ cm}^2\text{s}^{-1}$, $4.0 \times 10^{11} \text{ cm}^2\text{s}^{-1}$, $1.6 \times 10^{11} \text{ cm}^2\text{s}^{-1}$.

Table 1

The results of different modes for the case C1 with different R_Ω and $\eta_o (10^{11} \text{ cm}^2 \text{s}^{-1})$. Middle three columns show critical α -values (cm s^{-1}). The right three columns are the corresponding period (years) and phase shift between $A0$ and Sm . Bold is used when the mode has the smallest α -value.

R_Ω	Critical α			Period T & Phase shift		
	500	2000	5000	500	2000	5000
η_o	16.0	4.0	1.6	16.0	4.0	1.6
$A0$	104.8	9.91	1.6	1.85	6.8	16.88
$S1$	74.85	6.70	2.1	12.18	286.9	7347.7
				0.84π	0.69π	1.04π
$S2$	73.60	10.77	4.2	35.33	1207.6	3764.5
				1.30π	0.16π	1.33π
$S3$	82.56	15.55	6.4	71.75	7409.4	1742.5
				0.48π	0.79π	1.70π

Table 2

The same as Tab. 1, but for Case 2.

R_Ω	Critical α			Period T & Phase shift		
	500	2000	5000	500	2000	5000
η_o	16.0	4.0	1.6	16.0	4.0	1.6
$A0$	88.0	5.89	0.95	4.55	17.31	43.06
$S1$	79.39	8.50	2.53	26.06	349.5	2170.3
				0.72π	0.73π	0.74π
$S2$	83.47	12.97	4.65	64.88	739.2	8024.5
				1.75π	1.00π	1.00π
$S3$	93.57	17.7	6.87	119.6	1524.6	22587.4
				1.05π	0.95π	0.42π

3.1 The comparisons of the critical α -values among the different modes

The middle three columns of Table 1-3 show the critical α -values for different R_Ω and η_o of the case C1 that the α -effect concentrates in the tachocline ($r_a=0.675$, $r_b=0.725$ and $d=0.025$), C2 that the α -effect exists through the entire CZ ($r_a=0.7$, $r_b=1.0$ and $d=0.05$) and C3 that the α -effect locates at the top of the surface ($r_a=0.95$, $r_b=1.0$ and $d=0.025$), respectively. The modes

Table 3

The same as Tab. 1, but for Case 3 and critical α -values (m s^{-1}).

R_Ω	Critical α			Period T & Phase shift		
	500	2000	5000	500	2000	5000
η_o	16.0	4.0	1.6	16.0	4.0	1.6
$A0$	26.17	5.99	1.63	5.79	1.16	2.0
$S1$	16.77	4.55	1.88	0.297	0.293	0.292
				0.10π	1.10π	0.7π
$S2$	17.84	4.99	2.11	0.150	0.147	0.146
				0.10π	0.10π	1.29π
$S3$	19.12	5.46	2.22	0.101	0.100	0.099
				0.72π	0.25π	1.27π

with the lowest critical α -values are shown in bold.

The general rule that the larger m is, the more difficult the mode to excite is only satisfied when R_Ω is large enough and the corresponding diffusivity is lower enough. For example, when $R_\Omega = 5000$ ($\eta_o = 1.6 \times 10^{11} \text{ cm}^2\text{s}^{-1}$) for all of the three cases and $R_\Omega = 2000$ ($\eta_o = 4 \times 10^{11} \text{ cm}^2\text{s}^{-1}$) for C2 and C3, the models will favor the axisymmetric mode $A0$. However, when the turbulent diffusivity is strong ($\eta_o = 1.6 \times 10^{12} \text{ cm}^2\text{s}^{-1}$ for the three cases), the non-axisymmetric modes ($m = 2$ for C1, $m = 1$ for C2 and C3) have the lowest critical α -values and will be the preferred modes. Hence, the dynamo number R_Ω is the decisive parameter to select the dominant mode. According to $R_\Omega = \frac{|\Omega|_o R_\odot^2}{\eta_o}$, since the differential rotation is given, only the diffusivity in CZ contributes to the result and hence should be the key factor to the mode selection.

When R_Ω is large enough ($R_\Omega \gg R_\alpha$), the α -effect as the generation mechanism of toroidal field can be ignored and the $\alpha^2 - \Omega$ model is at the $\alpha - \Omega$ dynamo limit. At the $\alpha - \Omega$ limit, the axisymmetric mode ($m = 0$) which is the smallest wave number and has the largest scale field is least depressed by turbulent diffusivity and will be the preferred mode. When η_o increases and the corresponding R_Ω decreases, the ratio of R_Ω to R_α also decreases. The role of α -effect in generation of the toroidal field increases and the $\alpha^2 - \Omega$ model deviates the $\alpha - \Omega$ dynamo limit gradually. The more it deviates from the limit, the easier the non-axisymmetric modes are excited, which is in conformity with the asymptotic solution of Bassom et al. (2005).

The right three columns of Table 1-3 show the periods and phase shifts for

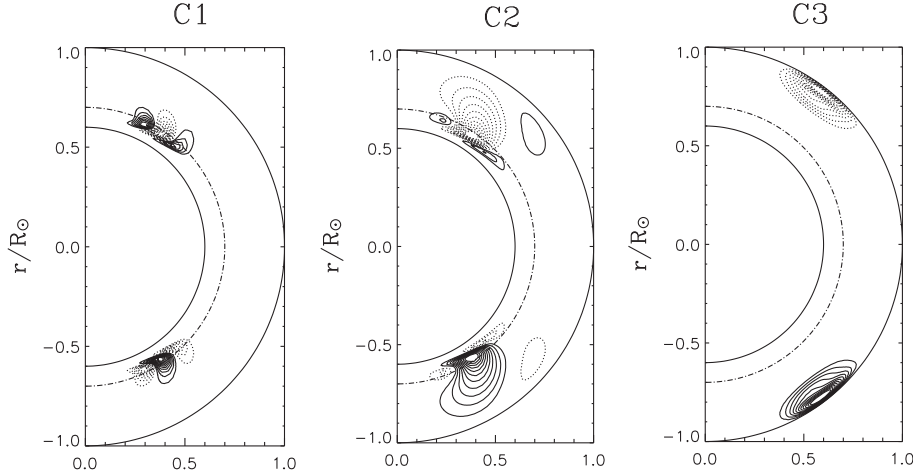


Fig. 2. Contours of the toroidal field B_ϕ of the axisymmetric mode $A0$ in a meridional plane with $R_\Omega=5000$ for the three cases with different locations of α -effects. Solid (dashed) contours correspond to positive (negative) magnetic field components. The dot-dashed lines locate at $0.7R_\odot$ marking the center of the tachocline. The radial distributions of the contour lines are consistent with that of the α -profiles. But the latitudinal locations which are around 55° latitude do not change with the α -profiles.

different modes with different R_Ω and η_o . For the axisymmetric mode $A0$ of the cases C1 and C2, it can be seen from the Table 1 and 2 that the period is nearly the inverse ratio of diffusivity and hence, is dominated by the diffusivity. The periods of the non-axisymmetric modes are much larger than that of $A0$. Therefore they are weakly oscillating or rather steady comparing with $A0$. This is consistent with observations (Berdyugina and Usoskin , 2003) and theory speculation (Fluri and Berdyugina , 2004). The co-existing of the two kinds of modes are used to explain active longitudes, flip-flops and other non-axisymmetric phenomena (Moss , 2004; Fluri and Berdyugina , 2004). In contrast, the oscillatory period of case C3 is much less than the other two cases. This is consistent with the independent results of (Ivanova and Ruzmaikin , 1985; Bigazzi and Ruzmaikin , 2004). The periods depend on the diffusivity much less especially for the non-axisymmetric modes. C3 is characterized by an α -effect which has no overlap with the shear layer. It probably is the reason to cause the difference. The meridional circulation neglected in our models should play much more important roles in C3 to determine the cycle.

Phase relation between the surface axisymmetric and non-axisymmetric poloidal field can be observed. Ruzmaikin et al. (2001) showed that there are about π -shift between the modes $A0$ and $S1$ and the nearly same phase between $S1$ and $S2$. The global phases (Schlichenmaier and Stix , 1995), based on the maximum values of B_r over the whole latitude ranges are computed. The phase shifts presented in Tab. 1-3 are the phase difference between $A0$ and Sm . The results dependent on R_Ω (η_o) and different cases. When R_Ω is large enough and diffusion is small, the phase shift can match the observation well.

3.2 The configurations of the magnetic fields for the three cases

Fig. 2 shows the contours of the toroidal field B_ϕ of the axisymmetric mode $A0$ in a meridional plane for the three cases when R_Ω is 5000. The centers of the contour lines concentrate at the nearly same high latitudes (about 55°) where have the strong radial shear. But the radial locations of the three cases are different. They are around the tachocline, throughout the whole CZ and near the surface respectively, which are consistent with the radial profile of the α -effects. Hence, the strong radial shear of the differential rotation and the α -effect play a dominant role in the form of the configuration of the axisymmetric fields.

Fig. 3 presents the distribution of B_ϕ of the distinguished non-axisymmetric modes for the three cases when R_Ω is 500. For C1 and C2, the magnetic field is highly concentrated in the lower part of the tachocline, where the diffusivity is small (see Eq. (9)). But it is different for C3 with the sub-surface α -effect. Moreover, for all the three cases, the non-axisymmetric fields are localized around 35° latitude where has the weakest radial shear (see left of Fig. 1).

The physical reason for the different localizations of the axisymmetric and non-axisymmetric modes can be understood from MHD theory (Moffatt , 1978). The differential rotation affects the two kinds of fields in different ways. It distorts the axisymmetric poloidal field perpendicular to the axis of rotation to form the axisymmetric toroidal field. By the way, this needs the non-zero diffusivity to assure the development of net toroidal flux. For the non-axisymmetric ingredients, they will be expelled from the strong differential rotating high-diffusivity region.

4 Conclusions and Discussion

By the comparisons of critical α -values among the modes $m \leq 3$ for a wide range of turbulent diffusivity and dynamo number R_Ω accordingly, we obtain that dynamo number R_Ω is the decisive parameter for the modes selection. When R_Ω is large enough, the dominant axisymmetric mode would be favored. With the decreasing of R_Ω , different non-axisymmetric modes will be preferred. Since R_Ω is the ratio of the differential rotation to magnetic diffusivity, both of the two ingredients should contribute to the modes selection. The role of differential rotation and its physical mechanisms have been well-known that the strong value prefers the axisymmetric mode. For the definite differential rotation given by helioseismology, the comparisons approve of the effect of the diffusivity in the mode selection and indicate that it is just contrary to the differential rotation. In other words, the strong turbulent diffusivity favors

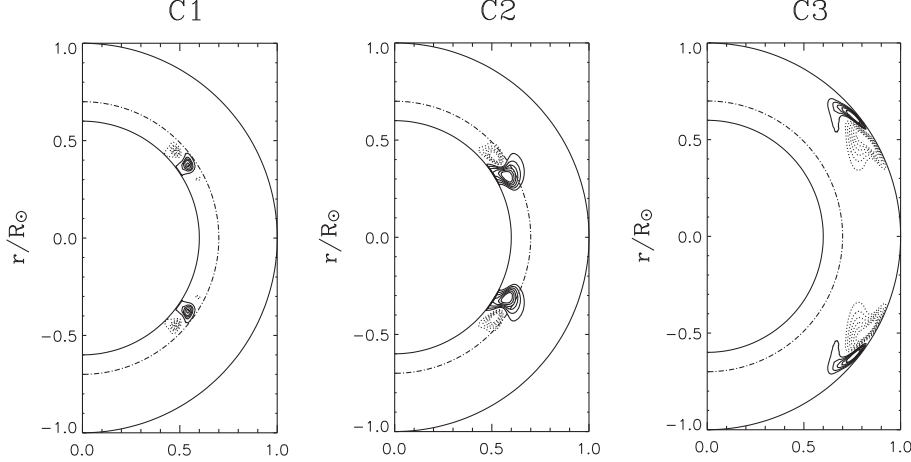


Fig. 3. Contours of the toroidal field B_ϕ of the non-axisymmetric modes in a meridional plane with $R_\Omega=500$ for the three different cases. The line styles are the same as in Fig 2. For C1 and C2, the field concentrates in the low diffusivity (below the dot-dashed line $0.7R_\odot$) and weak differential rotation (about 35° latitude). For C3, it has the same latitudinal location but concentrates near the surface.

the non-axisymmetric modes for the given rotation system of the Sun. On the other hand, the dominant mode given by the observation can be an important index to infer the inner turbulent diffusivity of the Sun or a star. What we have done is based on a linear non-axisymmetric $\alpha^2 - \Omega$ dynamo model in a rotating spherical frame which incorporates the solar-like differential rotation, the magnetic diffusivity varied with depth and three possible cases of the α -effects.

On the actual Sun, it is rather than a single preferred mode. The whole physics during the dynamo process is not only the interaction between magnetic field and turbulent velocity field but also the interaction between the various modes. The latter may lead to a stationary field amplitude and to a certain spectral distribution, even if the α -value is supercritical (Stix , 1971). The nonlinearities, such as a non-axisymmetric distribution of the α -effect (Moss et al. , 2002; Bigazzi and Ruzmaikin , 2004) and the α -quenching (Moss , 1999), induce the different modes coupled together. The non-axisymmetric enhancement of the underlying magnetic field causes in the clustering of sunspots to form active longitudes (Ruzmaikin , 2001).

Since the magnetic diffusivity is a diffusion of a vector field, the diffusivity profile should be expressed by a tensor. Yoshimura et al. (1984a ,1984b, 1984c) adopted the tensors for the diffusivity and demonstrated that it had close relations with parity selection. With a scalar expression, the growth rates for the odd and even parity modes are nearly the same (Seenbeck and Krause 1969; Deinzer and Stix 1971) which also been demonstrated by our code. But in the paper, the scalar diffusivity is still used for two reasons. One is for the simplicity. We do not refer to the parity problem and only adopt the odd par-

ity for axisymmetric mode and even parity for the non-axisymmetric modes. The other is limitation of the observations. The measurements of magnetic diffusivity inside of the Sun are not possible nowadays. Hence it is difficult to give its detailed distribution.

The configurations of the toroidal fields for the axisymmetric and non-axisymmetric modes are different. The former prefers to locate at the strong radial shear region and the latter favors the weak radial shear and low diffusivity regions. These are caused by the different roles that the differential rotation and diffusivity played in the two kinds of modes. Furthermore, the meridional circulation is not considered in the work. It plays an important role in the axisymmetric mode (Nandy and Choudhuri , 2002). It carries the strong axisymmetric toroidal field produced at the high latitudes to the low ones and produces the active regions there with the magnetic buoyancy. We will discuss its influence on the non-axisymmetric field in the coming papers.

Acknowledgments

We thank the reviewers, Arnab Rai Choudhuri and another anonymous one, for useful comments that resulted in improvements of our paper. We are grateful to Liao, X.H. for his careful supervision on the development of the numerical code. This work has been supported by National Natural Science Foundation of China (10573025, 10603008) and by the National Key Basic Research Science Foundation (G2006CB806303).

References

Altschuler, M.D., Trotter, D.E., Newkirk, G.Jr., Howard, R. The large-scale solar magnetic field. *Sol. Phys.* 39, 3-17, 1974.

Bai, T. Distribution of flares on the sun - Superactive regions and active zones of 1980-1985. *Astrophys. J.* 314, 795-807, 1987.

Bassom, A.P., Kuzanyan, K.M., Sokoloff, D., Soward, A.M. Non-axisymmetric $\alpha^2\Omega$ -dynamo waves in thin stellar shells. *Geophys. Astrophys. Fluid Dynam.* 99, 309-336, 2005.

Berdyugina, S.V., Usoskin, I.G. Active longitudes in sunspot activity:century scale persistence. *Astron. Astrophys.* 405, 1121-1128, 2003.

Bigazzi, A., Ruzmaikin, A. The sun's preferred longitudes and the coupling of magnetic dynamo modes. *Astrophys. J.* 604, 944-959, 2004.

Carrington, R.C. *Observations of spots on the Sun.* London: Williams and Norgate. 1863.

Castenmiller, M.J.M., Zwaan, C., van der Zalm, E.B.J. Sunspot nests - Manifestations of sequences in magnetic activity. *Sol. Phys.* 105, 237-255, 1986.

Charbonneau, P., Christensen-Dalsgaard, J., Henning, R. et al. Helioseismic constraints on the structure of the solar tachocline. *Astrophys. J.* 527, 445-460, 1999.

Chatterjee, P., Nandy, D., Choudhuri, A.R. Full-sphere simulations of a circulation-dominated solar dynamo. *Astron. Astrophys.* 427, 1019-1030, 2004.

de Toma, G., White, O.R., Harvey, K.L. A picture of solar minimum and the onset of solar cycle 23. *Astrophys. J.* 529, 1101-1114, 2000.

Deinzer, W., Stix, M. On the eigenvalues of Krause-Steenbeck's solar dynamo. *Astron. Astrophys.* 12, 111-119, 1971.

Dikpati, M. and Charbonneau, P. Babcock-Leighton flux transport dynamo with solar-like differential rotation. *Astrophys. J.* 518, 508-520, 1999.

Fluri, D.M., Berdyugina, S.V. Flip-flop as observational signatures of different dynamo models in cool stars. *Sol. Phys.* 224, 153-160, 2004.

Ivanova, T.S., Ruzmaikin, A. Three-dimensional model for generation of the mean solar magnetic field. *Astro. Nach.* 306, 177-186, 1985.

Jiang, J., Wang, J. X. A non-axisymmetric spherical α^2 dynamo model. *Chin. J. Astron. Astrophys.* 6, 227-236, 2006."

Moffatt, H.K. Magnetic field generation in electrically conducting fluids. Cambridge Univ. 1978.

Moss, D. Non-axisymmetric solar magnetic field. *Mon. Not. Roy. Astron. Soc.* 306, 300-306, 1999.

Moss, D. Dynamo models and flip-flop phenomenon in late-type stars. *Mon. Not. Roy. Astron. Soc.* 352, L17-L20, 2004.

Moss, D., Piskunov, N., Sokoloff, D. Non-axisymmetric cool spot distributions and dynamo action in close binaries. *Astron. Astrophys.* 396, 885-893, 2002.

Mursula, K., Hiltula, T. Systematically asymmetric heliospheric magnetic field. *Sol. Phys.* 224, 133-143, 2004.

Nandy, D., Choudhuri, A.R. Explaining the latitudinal distribution of sunspots with deep meridional flow. *Science*, 296, 1671-1673, 2002.

Parker, E.N. Hydromagnetic dynamo models. *Astrophys. J.* 122, 293-314, 1955.

Ruzmaikin, A. Origin of sunspots. *Space Sci. Rev.* 95, 43-53, 2001.

Ruzmaikin, A., Feynman, J., Neugebauer, M., Smith, E.J. Preferred solar longitudes with signatures in the solar wind. *J. Geophys. Res.* 106, 8363-8370, 2001.

Schlütermaier, R., Stix, M. The phase of the radial mean field in the solar dynamo. *Astron. Astrophys.* 302, 264-270, 1995.

Song, W.B., Wang, J.X. The differential rotation and longitudinal distribution of solar magnetic flux. *Astrophys. J.* 624, L137-L140, 2005.

Steenbeck, M., Krause, F., Rädler, K.H. A calculation of the mean electromotive force. *Z. Naturforsch.*, 21a, 369-376, 1966.

Steenbeck, M., Krause, F. On the dynamo theory of stellar and planetary

magnetic fields. *Astr. Nach.* 291, 49-84, 1969.

Stix, M. A non-axisymmetric α -effect dynamo. *Astron. Astrophys.* 13, 203-208, 1971.

Švestka, Z., Simon, P. Proton Flare Project, 1969. *Sol. Phys.* 10, 3-59, 1969.

Yoshimura, H., Wang, Z.Z., Wu, F. Linear astrophysical dynamos in rotating spheres Differential rotation. *Astrophys. J.* 280, 865-872, 1984.

Yoshimura, H., Wang, Z.Z., Wu, F. Linear astrophysical dynamos in rotating spheres. *Astrophys. J.* 283, 870-878, 1984.

Yoshimura, H., Wu, F., Wang, Z.Z. Linear astrophysical dynamos in rotating spheres. *Astrophys. J.* 285, 325-338, 1984.

Schou, J., Antia, H.M., Basu, S. Helioseismic studies of differential rotation in the solar envelope. *Astrophys. J.* 505, 390-417, 1998.

Schubert, G., Zhang, K.K. Effects of an electrically conducting inner core on planetary and stellar dynamo. *Astrophys. J.* 557, 930-942, 2001.